

In Vivo siRNA Delivery Using JC Virus-like Particles Decreases the Expression of RANKL in Rats

Daniel B Hoffmann¹, Kai O Böker², Stefan Schneider², Ellen Eckermann-Felkl², Angelina Schuder², Marina Komrakova¹, Stephan Sehmisch¹ and Jens Gruber²

Bone remodeling requires a precise balance between formation and resorption. This complex process involves numerous factors that orchestrate a multitude of biochemical events. Among these factors are hormones, growth factors, vitamins, cytokines, and, most notably, osteoprotegerin (OPG) and the receptor activator for nuclear factor- κ B ligand (RANKL). Inflammatory cytokines play a major role in shifting the RANKL/OPG balance toward excessive RANKL, resulting in osteoclastogenesis, which in turn initiates bone resorption, which is frequently associated with osteoporosis. Rebalancing RANKL/OPG levels may be achieved through either upregulation of OPG or through transient silencing of RANKL by means of RNA interference. Here, we describe the utilization of a viral capsid-based delivery system for *in vivo* and *in vitro* RNAi using synthetic small interfering RNA (siRNA) molecules in rat osteoblasts. Polyoma JC virus-derived virus-like particles are capable of delivering siRNAs to target RANKL in osteoblast cells both *in vitro* and in a rat *in vivo* system. Expression levels were monitored using quantitative real-time polymerase reaction and enzyme-linked immunosorbent assay after single and repeated injections over a 14-day period. Our data indicate that this is an efficient and safe route for *in vivo* delivery of gene modulatory tools to study important molecular factors in a rat osteoporosis model.

Molecular Therapy—Nucleic Acids (2016) 5, e298; doi:10.1038/mtna.2016.15; published online 22 March 2016

Subject Category: siRNA, shRNA and miRNAs; Nanoparticles

Introduction

Osteoporosis is a widespread disease, and due to an aging society, the incidence of osteoporosis and osteoporosis-associated bone fractures is increasing. Thus, osteoporosis represents one of the most challenging diseases today and for the future. Bone metabolism and plasticity are regulated largely by the interaction of two skeletal cell types, osteoblasts and osteoclasts. A disruption in the balance of osteoblastic bone formation and osteoclastic bone resorption is one of the key mediators of the onset of osteoporosis.¹ Numerous factors, including cytokines, hormones, growth factors, and, in particular, osteoprotegerin (OPG) and the receptor activator for NF- κ B (RANK) ligand precisely orchestrate bone resorption and formation.² Recent studies have suggested a decisive role for the RANK/RANKL/OPG system in regulating bone metabolism.^{3,4} RANK is present in osteoclasts, where it promotes osteoclastogenesis upon binding to RANK ligand (RANKL), produced by osteoblasts and other stromal cells. OPG acts as a decoy receptor by binding to RANKL and preventing RANK signaling. Osteoclast activation is thus blocked and apoptosis induced.⁴ However, elevated levels of OPG in serum have recently been shown to be associated with an increased risk of cardiovascular disease.^{5,6} Therefore, it would seem more promising for (bone) metabolism to reduce the amount of RANKL expression rather than to increase OPG.

Addressing the balance of RANKL and OPG can be achieved by a number of techniques, including targeting

accessible soluble or membrane-bound RANKL with specific antibodies, increasing OPG levels through delivery of exogenous expression constructs or transiently reducing the amount of RANKL using RNA interference (RNAi).^{7–9}

Denosumab (AMGen, Thousand Oaks, CA) is a newly approved drug for the treatment of osteoporosis. It is a fully human monoclonal antibody against RANKL (receptor activator of nuclear factor- κ B ligand) that reversibly inhibits bone resorption by reducing both osteoclast formation and differentiation and increasing osteoclast apoptosis. Denosumab is well tolerated; however, adverse side effects (osteonecrosis of the jaw, musculoskeletal pain, eczema, etc.) can occur,¹⁰ at which time treatment should be discontinued. This could be problematic, as the effects of denosumab wear off about 6 months after the last injection. Furthermore, the agents that block the RANKL–RANK interaction may cause side effects due to the lack of specificity, and the involvement of the RANKL/RANK/OPG system in a variety of other biological processes, including the immune response. Therefore, better strategies need to be developed for targeting the RANKL/RANK/OPG system more specifically and effectively.¹¹ Intense investigations into RANKL signaling have identified TRAF-binding motifs (PFQEP^{369–373}; PVQEET^{559–564}; and PVQEQG^{604–609}) and a TRAF-independent motif (IVVY^{535–538}) in the cytoplasmic domain of RANK, which have a role in osteoclastogenesis.¹¹

In the current study, we have established a basis for the re-balancing approach by applying small interfering RNAs

The first two authors contributed equally to this work.

¹Department of Trauma Surgery and Reconstructive Surgery, University Medical Center Göttingen, Göttingen, Germany; ²Primate Genetics Laboratory, Junior Research Group "Medical RNA Biology," German Primate Center, Göttingen, Germany. Correspondence: Jens Gruber, Junior Research Group "Medical RNA Biology," Deutsches Primatenzentrum GmbH (German Primate Center), Kellnerweg 4, 37077 Göttingen, Germany. E-mail: jgruber@dpz.eu

Keywords: *in vivo*; osteoporosis; RANKL; RNAi; siRNA delivery; virus-like particles

Received 26 October 2015; accepted 4 February 2016; published online 22 March 2016. doi:10.1038/mtna.2016.15

(siRNA) to reduce the amount of expressed RANKL. However, all *in vivo* therapies utilizing synthetic siRNAs face the problem of delivery—that is, the transfer of the RNAi-inducing molecule to the relevant cell type, while keeping possible off-target effects to a minimum. RNAi is a well-characterized mechanism for both the transcriptional and posttranscriptional regulation of gene activity. In particular, siRNAs are an efficient and easily applied tool to mediate the posttranscriptional degradation of target mRNA molecules in a highly sequence-specific manner.^{9,12}

Utilization of synthetic siRNAs *in vivo* with the goal of a transient reduction in gene expression was applied in various modes, including “naked” siRNAs, lipid-based complexes, or chemically modified siRNAs attached to biomolecules with a specific affinity for the respective target tissues.^{13,14} Other approaches included following viral delivery routes for the expression of short hairpin RNAs to induce silencing of the target genes.^{15–17}

The human polyoma JC virus VP1 protein can be utilized as a gene or nucleic acid delivery vehicle to transfer effector molecules into cells bearing the suitable entry receptors.^{18,19} Cellular entry is mediated through binding and internalization of glycolipids and sialoglycoproteins, including LSTc-binding, and by interaction with the specific serotonin receptor, 5-hydroxytryptamine-receptor 2a.^{20–22} The effective transfer of genetic material in virus-like particles (VLPs) has been reported using a recombinant VP1 protein generated in *Escherichia coli* bacteria.^{8,19}

In the present study, we attempted to establish a method for re-balancing RANKL and OPG levels by applying siRNAs to reduce the amount of expressed RANKL, using the recombinant human polyoma JC virus VP1 protein as a delivery system.

Results

Validation of a VLP-based delivery approach

The delivery of tools to manipulate gene expression into cells that produce RANKL was the most important step toward *in vivo* utilization of systemically applied RNAi. We chose to work with polyoma JC-derived virus like particles because of the ease of production and purification. In addition, it is possible to load nucleic acids into the lumen of VLPs *in vitro* by disassembling and reassociating the particles in the presence of siRNAs. Recombinant VLPs are composed of a recombinant VP1 protein from the human polyoma JC virus. The VP1 protein was produced in insect cells using a baculoviral expression system (Figure 1a). Purified VP1 protein spontaneously forms stable homo-pentameric capsomers, which in turn assemble into VLPs. Electron-micrographs (Figure 1b) show 40-nm-diameter VP1 VLPs, consisting of 72 capsomers after the purification procedure. Reducing conditions allow the disassembly of VLPs, opening their structure and making it accessible to cargo, such as synthetic nucleic acids like siRNAs. Empty and filled particles are shown for comparison (Figure 1b). Refolding of the capsids by dialysis in physiological salt and pH conditions results in VLPs that contain siRNAs. This is largely due to the fact that the inner surface of VLPs has an affinity for the negatively charged phosphate backbone of nucleic acids. Figure 1c shows the dissociation/reassociation cycle for siRNA loading, which was performed *in vitro* with purified recombinant VP1 VLPs

and synthetic siRNA molecules. We routinely used a weight ratio of 0.074 µg siRNA per 1 µg VP1 VLP, reflecting around 74.5 siRNA molecules per VLP. The detailed calculation of weight and molar ratios is provided in the **Supplementary Material**. Considering only the inner volume of a VLP sphere, the theoretical threshold is a load of 1,217 siRNAs. However, only around 300 siRNAs can possibly interact directly with the inner surface. Considering these calculated values, we have achieved fourfold excess of VLPs over siRNAs and have highly efficient packaging of the siRNAs, which leaves hardly any free siRNA molecules after the *in vitro* reassociation process. This was confirmed by an electrophoretic mobility shift assay in which we did not observe any free siRNA after the packaging procedure (**Supplementary Figure S2**).

A comparison of the primary amino acid sequences of the human and the rat serotonin receptor 2a (5-hydroxytryptamine-2A, HTR2a) displays a high degree of conservation and a high level of identity among the two proteins, with 91% identical and 95% positive matching residues (Figure 2a). High expression levels of HTR2a on osteoblast cells have previously been described²³ and are considered to be an entry point for the human JC virus-based VLPs. In particular, the N-linked glycosylation sites in the extracellular amino-terminal region of HTR2a are conserved between rat and human. We investigated the expression of HTR2a on cell lines and in primary bone material from tibiae and lumbar vertebrae of untreated rats to assure interaction opportunities for the JC-VLPs. In both cultured osteoblasts and in cDNAs from the bone material, we observed strong expression of HTR2a at the mRNA level (**Supplementary Figure S1**).

Rat osteoblasts were cultured as previously described^{24,25} and were terminally differentiated prior to treatment with VLPs. Differentiation of the osteoblast cell line was induced by adding dexamethasone, glycerophosphate, and vitamin C to the standard culture medium. The cellular uptake of VLPs was monitored via fluorescence- (Cy3) labeled small RNAs that were loaded as a cargo. Delivery into rat osteoblasts was successful and reached over 90% of the cells (Figure 2b). The onset of cell binding occurred after 4 hours, indicating a high affinity of the VLPs for the surface of the rat osteoblasts (**Supplementary Figure S3**). The functionality of the siRNAs, and therefore RNA release, was subsequently confirmed by delivering siRNAs targeting the mitosis-related kinesin motor protein KIF11 (rat Eg5), which resulted in apoptosis in ~40% of the cells 44 hours after VLP treatment (**Supplementary Figure S3**, bottom panel). Various alternative methods have been utilized to screen for delivery efficiency, including VLPs in combination with transferrin-conjugated poly-ethyleneimine (PEI-Tf), PEI-Tf alone, and two different transfection reagents for lipofection. Delivery was comparably efficient for VLPs with and without PEI-Tf, reaching over 90% of the cells, while all other techniques were less efficient, resulting in only 3–15% transfected cells (**Supplementary Table S1**).

Based on the positive findings for VLP-mediated delivery, we selected one efficient siRNA targeting the rat RANKL-gene for the RNAi-based gene-silencing experiments. The knockdown of RANKL was evaluated at the mRNA level by quantitative real-time polymerase reaction (qPCR) and at the protein level by western blotting of protein extracts from osteoblasts, including conditioned media. Cells were terminally differentiated before

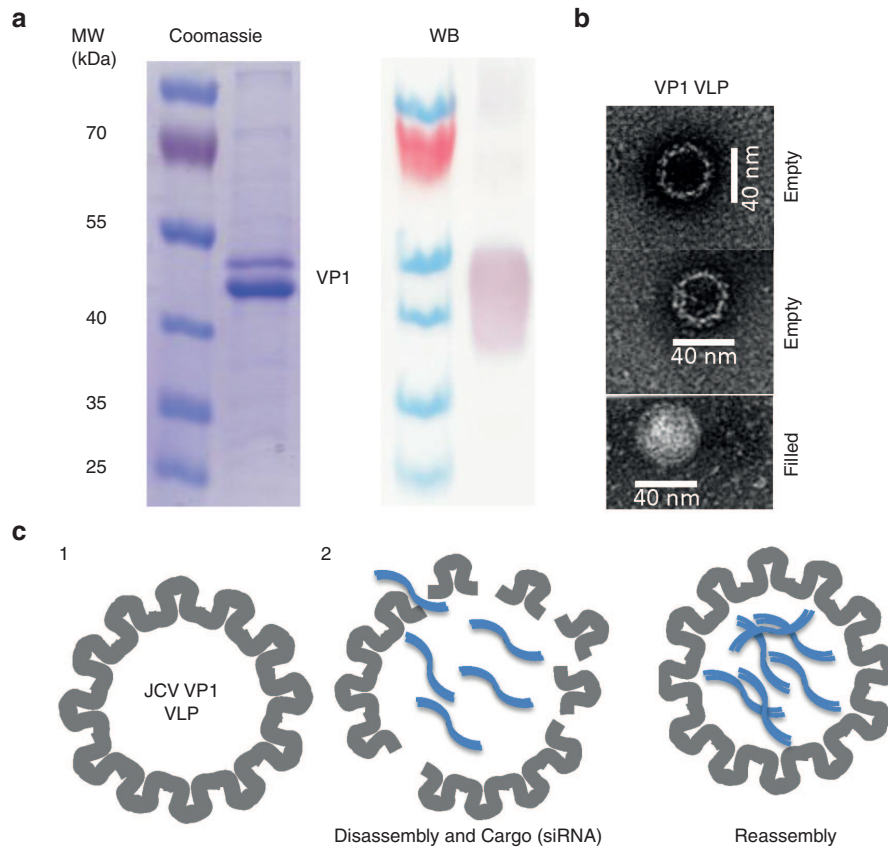


Figure 1 Production and assembly of siRNA-filled polyoma JCV VP1 VLPs. Images in (a) display purified JCV VP1 protein in sodium dodecyl sulfate polyacrylamide gel electrophoresis gels after Coomassie stain and western blot with VP1 antibody. The double band of VP1 at 45 and 47 kDa reflects two stages of posttranslational modification, while both bands are bigger than the calculated molecular weight of about 40 kDa. Western blot confirmed the identity of VP1, displaying saturated signals for small volumes of VP1-solution (here 1 μ l). (b) Electron micrographs of VLPs display spherical capsids with an outer diameter of 40 nm. Empty and (siRNA) filled VLPs can be distinguished. Bottom panel in (c) shows a sketch of *in vitro* VLP-loading in a single dissociation–reassociation cycle. Purified recombinant VP1 VLPs form capsids with a diameter of around 40 nm (1) that can be disassembled into capsomers (VP1-pentamers) in reducing conditions (2). In the dissociated stage, cargo-siRNAs can be added and VLPs can form around the nucleic acid cargo during slow dialysis versus physiological, nonreducing buffer conditions.

transfection or VLP-mediated transduction with the synthetic siRNAs or with controls. Both siRNAs successfully reduced the products of the target gene, in unmodified VLPs as well as in PEI-Tf decorated VLPs. Knockdown efficiency was in the range of 60–90% at the mRNA level, and reduced protein levels were observed by western blot (Figure 3). In particular, the efficiency of un-decorated (no PEI-Tf) VLPs with their native tropism indicated a promising application option for *in vivo* delivery into test animals. Although VLPs with an external PEI-transferrin decoration were more efficient at silencing RANKL, one must consider the increased cell death rates that occurred in the presence of the polymer. In contrast, no cytotoxic effects were observed in cells that were treated with siRNA-filled VLPs without further modifications on the outer surface. Thus, we utilized VLPs and loaded RANKL siRNAs to identify suitable conditions for the RNAi approach in living animals.

***In vivo* application of VLPs for siRNA delivery**

Following the work in tissue culture and cell lines, we proceeded to apply the VLP technology *in vivo*, to adult female rats. In the first experiment, we studied the general effects of toxicity for three injection routes using a control-RNA cargo,

namely *i.p.*, *i.v.*, and *i.m.*. Animals were kept for 3 days after the injection of 10, 50, or 100 μ g of VLPs via the respective routes and then were sacrificed to determine pathological defects. None of the injection routes resulted in adverse effects, and no obvious macroscopic pathological defects were observed (data not shown). Also, in subsequent experiments, we never observed clinical symptoms in the VLP-injected animals, and none of the rats died before the scheduled sacrifice. Only one rat died before being euthanized, but this animal received an *i.p.* injection of buffer only.

A proper perfusion for systemic delivery is required, and therefore, we selected *i.p.* injection as the preferred route for VLP delivery. The outcomes of the individual experiments with adult female rats are summarized in Table 1.

VLP-mediated siRNA delivery is dose dependent

For the first set of silencing experiments, we injected low (40 μ g VLP/animal, 3 μ g of siRNA), medium (105 to 120 μ g/animal, 7.8 or 8.9 μ g of siRNA, respectively), or high (150 μ g/animal, 11.2 μ g of siRNA) doses of siRNA-loaded VLPs (reflecting 0.14, 0.38, or 0.52 mg VLP per kg body weight) and examined RANKL mRNA levels in bone material from

a Alignment of 5-hydroxytryptamine receptor 2A from rat and human

Score	Expect	Method	Identities
887 bits(2293)	0.0	Compositional matrix adjust.	430/471(91%)
Rat 1	MEILCEDNISLSSIPNSLMQLGDGPRLYHNDFNSTRDANTSEASNWTIDAENRTNLSCEGY		60
Human 1	M+ILCE+N SLSS NSLMQL D RLY NDFNS +ANTS+A NWT+D+ENRTNLSCEG		60
Rat 61	MDILCEENTSLSSTTNSLMQLNDDTRLYSNDFNSGEANTSDAFNWTVDSENRTNLSCEGC		60
Rat 61	LPPTCLSILHLQEKNSALLTTVVIILTIAGNIIIVIMAVSLEKKLQATNYFLMSLAIAID		120
Human 61	L P+CLS+LHLQEKNSALLT VVIILTIAGNIIIVIMAVSLEKKLQATNYFLMSLAIAID		120
Rat 121	LSPSCLSLHLQEKNSALLTAVVVIILTIAGNIIIVIMAVSLEKKLQATNYFLMSLAIAID		120
Rat 121	MLLGLFVMPVSMILTILYGYRWPLPSKLCIAWIYLDVLFSTASIMHLCAISLDRIYVAIQNP		180
Human 121	MLLGLFVMPVSMILTILYGYRWPLPSKLC+WIYLDVLFSTASIMHLCAISLDRIYVAIQNP		180
Rat 181	IHHSRFNSRTKAFLEKI IAVWTISVGI SMPI PVFGLQDDSKVFEKGSCLLADDFVLI GSF		240
Human 181	IHHSRFNSRTKAFLEKI IAVWTISVGI SMPI PVFGLQDDSKVFEKGSCLLADDFVLI GSF		240
Rat 241	VAFFIPLTIMVITYFLTIKSLQKEATLCVSDLSTRAKLASFSFLPQSSLSSEKLFQRSIH		300
Human 241	V+FFIPLTIMVITYFLTIKSLQKEATLCVSDL TRAKLASFSFLPQSSLSSEKLFQRSIH		300
Rat 301	VSFFIPLTIMVITYFLTIKSLQKEATLCVSDLSTRAKLASFSFLPQSSLSSEKLFQRSIH		300
Rat 301	REPGSYAGRRTMQSISNEQKACKVLGIVFFLVVMMWCPFFITNIMAVICKESCNE+VIGA		360
Human 301	REPGSYAGRRTMQSISNEQKACKVLGIVFFLVVMMWCPFFITNIMAVICKESCNE+VIGA		360
Rat 361	REPGSYAGRRTMQSISNEQKACKVLGIVFFLVVMMWCPFFITNIMAVICKESCNE+VIGA		360
Rat 361	LLNVFVWIGYLSAVNPLVYTLFNKTYRSAFSRYIQCCYKENKPLQLILVNTIPALAYK		420
Human 361	LLNVFVWIGYLSAVNPLVYTLFNKTYRSAFSRYIQCCYKEN+KPLQLILVNTIPALAYK		420
Rat 421	LLNVFVWIGYLSAVNPLVYTLFNKTYRSAFSRYIQCCYKENKPLQLILVNTIPALAYK		420
Rat 421	SSQLQVGGKKNQEDAEQTVDDCSMVTLGKQQSEENCTDNIETVNEKVSCV		471
Human 421	SSQLQ+GQKKN+DA+ T +DCSMV LGKQ SEE DN + VNEKVSCV		471
Human 421	SSQLQMGKKNKQDAKTTDNDCSMVALGKQHSSEASKDNSDGVNEKVSCV		471

Positives	Gaps
448/471(95%)	0/471(0%)

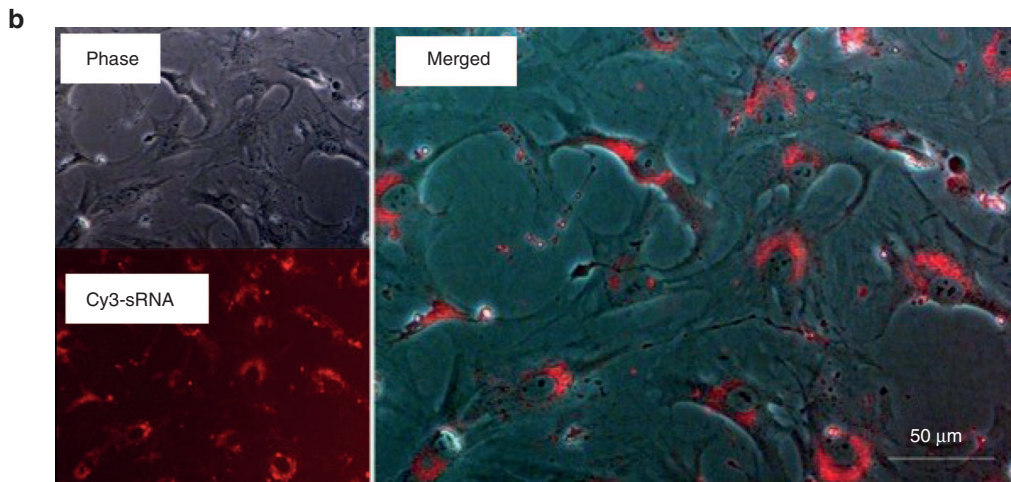


Figure 2 Sequence alignment of 5HT_{2A} receptors and cellular uptake of Cy3-RNA-containing VLPs into rat osteoblast cells. The alignment in (a) shows a comparison of the rat and human HT_{2A} receptor sequences. Both proteins show a high degree of similarity and all N-linked glycosylation sites that are required for interaction with JCV capsids are present in the rat molecule (shown in red). (b) Delivery of fluorescence-conjugated siRNAs in VLPs was tested in rat osteoblasts. Red fluorescence was observed 24 hours after VLP treatment, as documented using a fluorescence microscope (bar = 50 μm).

the tibia 72 hours after injection (compare Table 1). We observed no significant silencing effects for animals injected with NaCl, 120 μg VLPs with control RNA (siControl) or 40 μg VLPs with siRANKL. Injection of 120 μg siRANKL-VLPs reduced the target mRNA by 20%, while injection of 150 μg resulted in our goal of a 25–50% reduction in RANKL-mRNA and reached significance ($P = 0.0008$; Figure 4). This condition was therefore used in all of the subsequent experiments.

Statistical significance of *in vivo* RANKL silencing

After observing high fluctuations in the endogenous levels of RANKL mRNA in control animals, which caused difficulties in reaching confidence in the statistical analyses, we increased the number of animals in the control and effector groups. We examined the significance of the silencing effects after VLP-mediated siRNA delivery 72 hours post-injection. We performed two independent experiments with 15 animals (in total), 5 animals each for buffer injection, VLP-siControl,

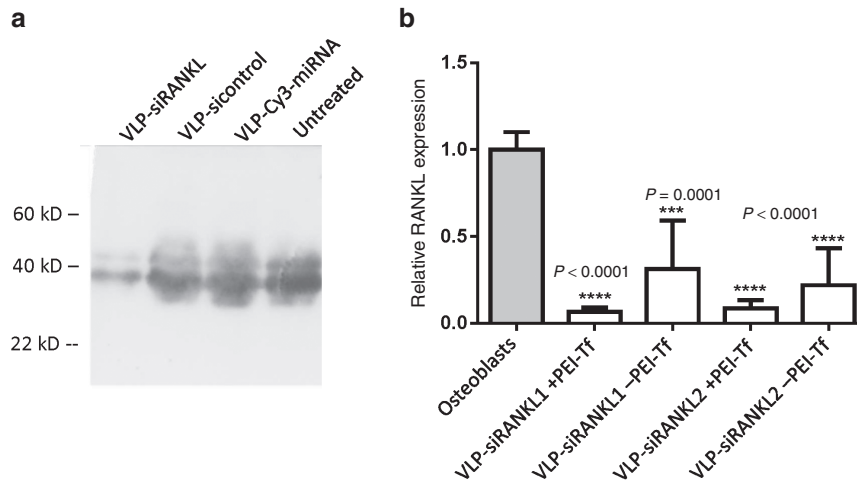


Figure 3 JCV VLP-mediated delivery of siRNA against RANKL in cultured cells. Differentiated rat osteoblasts were treated with VLPs containing siRNA against RANKL and assayed after 72 hours. (a) Reduced levels of RANKL protein could be seen following western blot analysis, indicating that treatment with VLPs successfully delivered siRNA cargo into the cells. Equal amounts of protein were loaded into each lane. qPCR of RANKL in (b) shown after delivering two different siRNAs in VLPs, with or without PEI-transferrin. Silencing efficiencies were between 60 and 90%, indicating a high rate of transduction with successful release of the siRNAs and a sufficient cellular uptake that is mediated by utilizing the transferrin receptor or the native JCV tropism via sialic acid (LSTc glycosylation) and HTR2a.

and VLP-siRANKL. Animals were euthanized after 3 days, and bones (tibia and lumbar vertebra) were extracted for qPCR. RANKL levels were quantified in RNA extracted from tibia and lumbar vertebra (Figure 5). Results from two experimental units is provided in the **Supplementary Figure S4**. Beta-2-microglobulin served as a reference gene for the normalization of RANKL levels and in the evaluation of silencing using the $\Delta\Delta C_t$ -method.²⁶ Normal Gaussian distribution of RANKL within the control groups was confirmed by a D'Agostino and Pearson test^{27,28} to qualify the datasets for statistical analysis using an unpaired *t*-test. At 72 hours after injection, RANKL mRNA levels were significantly reduced by 40% (tibia) or 23% (lumbar vertebra) with $P < 0.001$ and $P < 0.05$, respectively (Figure 5). RANKL-mRNA levels in lumbar vertebra and tibia of each animal from experiment 4 are provided in the **Supplementary Figure S5**.

Repeated VLP injections recover the silencing of RANKL

Since a longer-lasting effect (more than 3 days) would be required to study bone modeling dynamics *in vivo*, e.g., in terms of osteoporosis research and treatment, we performed a silencing kinetics study over 14 days and characterized RANKL mRNA and protein levels after 3 and 7 days for animals with a single VLP injection and after 14 days for animals that received a second injection after 7 days (Figure 6). In this experiment, we observed significant silencing of RANKL in the tibia after 3 days, but the levels ranged from a significant ($P < 0.05$) reduction of 76% back to 87% residual RANKL-mRNA, with nonsignificant values ($P = 0.064$) after 1 week (Figure 6). However, in the group of female rats that received a second injection, a silencing of ~30% was recovered, and the values reached significance ($P < 0.05$) again.

In addition to investigating effects on mRNA levels, we also quantified RANKL at the protein level using a specific enzyme-linked immunosorbent assay (ELISA) (**Supplementary Figure S6**). In bone material from the tibiae of

VLP-injected animals, we observed a reduction in RANKL that reflected the qPCR results from the same sample. A comparison of control animals and VLP-siRANKL-injected animals revealed a silencing of ~25% after 3 days that subsequently recovered to 85% of the control-animals' level. In the group of rats that received a second injection after 7 days and was examined after an additional 7 days, the average silencing of RANKL resembled the data obtained from the single injection 72 hour group. These results suggest that an adaptive silencing effect can be reached with repeated VLP injections. However, although the trends of silencing have been clearly documented and correlate with what was found at the mRNA level, statistical significance was not reached with the protein data. This is due to the enormous differences in the presence of RANKL-protein in the tissues of the test animals. SDs reached ~60% of the average values in the control group and therefore do not allow significance within the maximum 30% silencing window. However, RANKL levels appeared to become stabilized with reduced SDs on a lower level after the double VLP injection.

All data from the animal experiments are summarized in **Table 1**, indicating the repeated success of reducing endogenous RANKL mRNA levels by injecting RANKL-targeting siRNAs using VLPs as carrier complex.

Discussion

Polyoma JC VP1 VLPs mediate siRNA delivery both *in vitro* and *in vivo*

The utilization of polyoma JC based VLPs has previously been reported for gene transfer in tissue culture and cell lines^{18,19} and was shown to be an efficient method for the transduction of *in vitro* packaged DNA. Also, the delivery of encapsulated small molecules was demonstrated with propidium iodide as an example of pharmaceutical substances.²⁹ Effector molecules for the induction of target-specific RNAi have been delivered in JC VLPs, as was

Table 1 Summary of *in vivo* RNAi and VLP injection in female rats

Experiment number	Animals	Compound	Amount (VLP/injection)	Injection route	Time p.i.	Effect (silencing)	Significant	Comments	
1	3	VLP + Cy3-RNA	10, 50, 100 µg	i.m. (leg)	72 hours	None	n.a.	Test for toxicity	
	3			i.v. (tail)	72 hours				
	3			i.p.	72 hours				
2	2	Buffer		i.p.	72 hours	None	No	First effector test	
	2	VLP + Cy3-RNA	40 µg		72 hours	None	No		
	2	VLP + siRANKL	40 µg		72 hours	None	No		
	2	VLP + Cy3-RNA	120 µg		72 hours	None	No		
	2	VLP + siRANKL	120 µg		72 hours	ca. 15%	Yes ($P < 0.05$)		
3	5	Buffer		i.p.	72 hours	None	No	Significance test	
	5	VLP + Cy3-RNA	105 µg		72 hours	None	No		
	5	VLP + siRANKL	105 µg		72 hours	25%	Yes ($P < 0.05$)		
4	10	Buffer		i.p.	72 hours	None	No	Significance test 2	
	10	VLP + Cy3-RNA	150 µg		72 hours	None	No		
	10	VLP + siRANKL	150 µg		72 hours	27%	Yes ($P < 0.05$)		
5 kinetics experiment	7	VLP + Cy3-RNA	150 µg	i.p.	72 hours	None	No	Repeated injection after 7 days	
	7	VLP + Cy3-RNA	150 µg		7 days	None	No		
	7	VLP + Cy3-RNA	150 µg + 150 µg		14 days	None	No		
	7	VLP + siRANKL	150 µg		72 hours	29%	Yes ($P < 0.01$)		
	7	VLP + siRANKL	150 µg		7 days	15%	No ($P = 0.055$)		Recovered RANKL level
	7	VLP + siRANKL	150 + 150 µg		14 days	28%	Yes ($P < 0.05$)		Repeated injection after 7 days

demonstrated for short hairpin RNAs targeting transcripts of the polyoma BK virus.³⁰ The *in vivo* use of VLPs for the transduction of genetic material has so far only been shown for the inhibition of growth rates of human colon adenocarcinomas in a nude mouse model.⁸ The latter study involved *Escherichia coli*-derived *in vivo* DNA-packaged VLPs for the delivery. However, here we report for the first time the delivery of synthetic siRNAs both for *in vitro* and *in vivo* gene silencing in rats and in cell lines.

The VLP technology was successful in mediating siRNA-induced silencing of RANKL and KIF11 in differentiated rat-osteoblast cell lines. Silencing of the KIF11 gene was confirmed by observation of apoptotic cell death. Efficient silencing of RANKL was documented at both the mRNA and the protein level, and cytotoxic effects were not seen following either treatment with the VLPs or in the presence of siRNAs targeting RANKL mRNA.

The cellular uptake of VLPs is mediated by the cell surface markers, 5-HT₂ receptors, in particular HTR2a, and sialylated glycans (lactosierietetrasaccharide c, LSTc).^{22,31–33} These are present on both human and rat cells, and the HT2a receptor is involved in neurotransmitter-mediated dynamics of bone organization.^{34–36} Disturbing the serotonin signaling pathway was also shown to negatively influence bone formation and reduce bone accrual.^{37,38} We were able to recruit this system for the purpose of delivering effector molecules into osteoblast cells. Delivery of siRNAs against the RANKL gene efficiently silenced the target by 60–80%. Combining siRNA-loaded VLPs with PEI-transferrin that is complexed to the outer VLP-surface increased the silencing effect to over 90%. This was due to an increased and accelerated uptake of the VLPs via the transferrin receptor, which is expressed at high densities on most cell types. However, including PEI-Tf

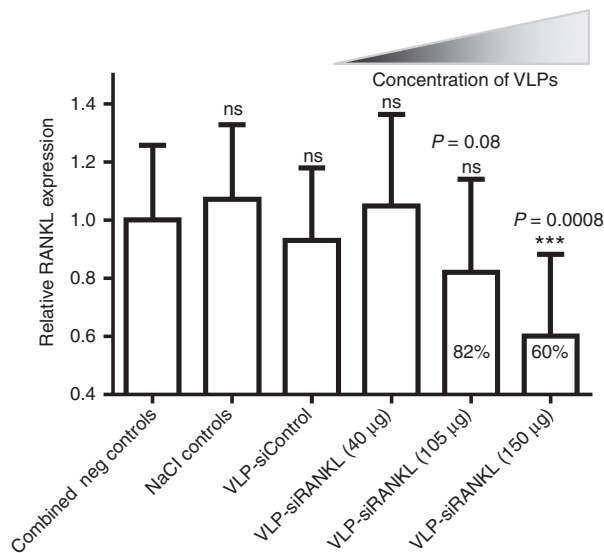


Figure 4 Dose-dependent reduction of RANKL mRNA in the tibiae of VLP-injected female rats. Adult female (wild type) Sprague Dawley rats received i.p. injections of buffer (saline), 120 µg of VLPs with control RNAs (siControl), and 40 µg (low), 105–120 µg (medium), or 150 µg (high) of VLPs containing the validated anti-RANKL-siRNA (siRANKL) in independent experimental units. After 72 hours, tibiae of euthanized animals were subjected to RNA extraction and subsequent qPCR to analyze RANKL mRNA levels. No silencing effects were observed for the saline, control RNA, or 40 µg animals, indicating that RANKL levels are not affected by injecting low doses of VLPs. Injecting 120 µg resulted in a reduction of ~18%, indicating a moderate knockdown effect without reaching significance ($P = 0.08$). The strongest and significant ($P < 0.001$) effect was seen in animals that received 150 µg of VLPs. Results were variable, but a clear knockdown of 25–50% was achieved.

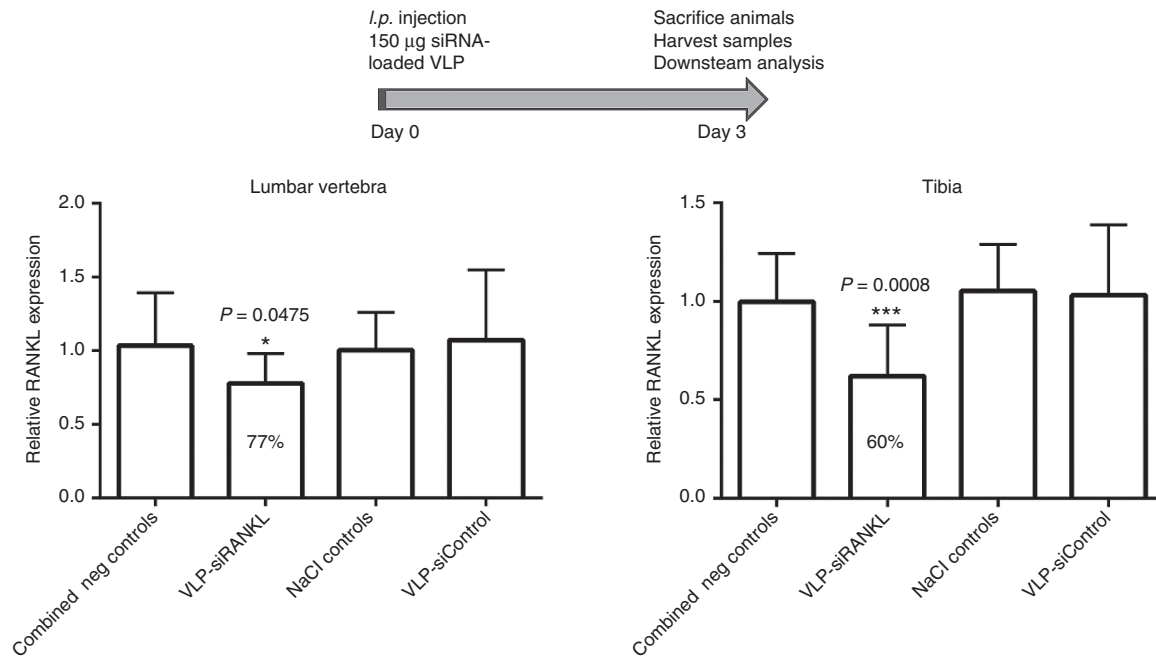


Figure 5 *In vivo* RNAi against RANKL in rat tibiae and lumbar vertebrae. Adult female rats received i.p. injections with buffer, 150 µg of VLPs containing control RNAs or VLPs with siRANKL and were euthanized after 3 days. Total RNA was extracted from the lumbar vertebra and tibia and subjected to quantitative real-time PCR. Expression levels of RANKL mRNA were normalized to β -2-microglobulin and a Gaussian distribution of expression levels was confirmed by a D'Agostini and Pearson test. Significant silencing of RANKL was observed in lumbar vertebrae (23% reduction) and tibiae (40% reduction).

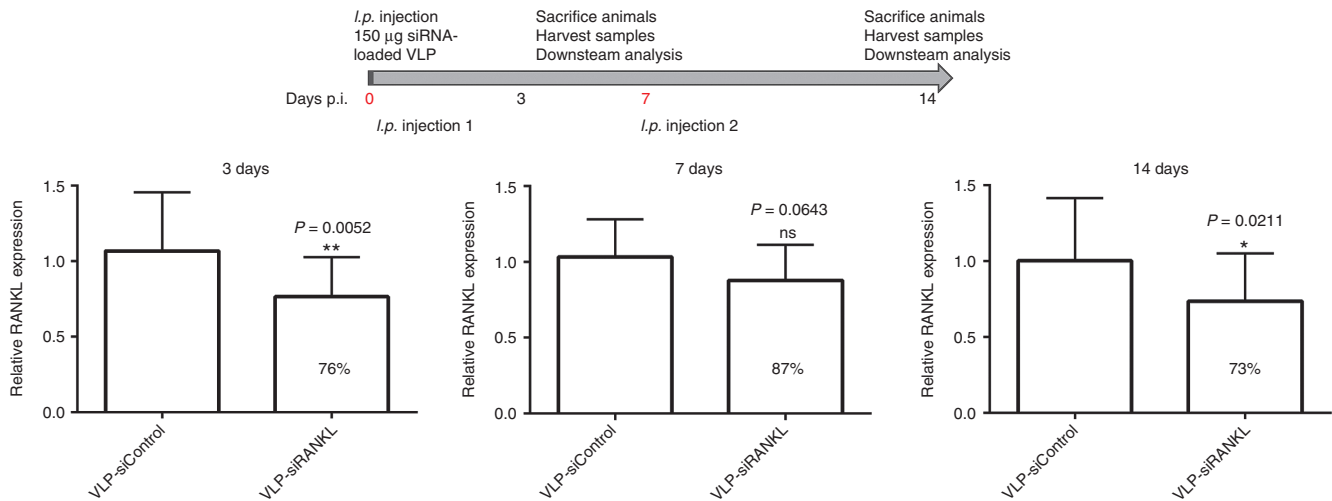


Figure 6 Kinetics of RANKL silencing after single and repeated VLP injections. Groups of seven adult female Sprague Dawley rats were assembled each for single injection of VLPs with siRANKL or control RNA. RANKL mRNA levels in extracted bone material from tibiae were examined after 3 or 7 days. Two groups (siRANKL and control) received a second injection with the respective VLP formulation after 7 days and were kept for another 7 days until examination of RANKL mRNA. Reduced values were observed after 72 hours, with silenced RANKL mRNA down to 70% of the control population. After 7 days, the level recovered to more than 80% of the control. The second injection of VLPs restored the RANKL silencing and prolonged the knockdown effect when measured after another 7 days (*i.e.*, 14 days after the initial i.p. injection of VLPs).

in the delivery experiments also induced cytotoxic effects and reduced the ratio of viable cells to 80% and may have caused some side effects, while reducing RANKL mRNA levels at the same time. Therefore, due to the very abundant expression of transferrin receptors, we did not use PEI-Tf-complexed VLPs *in vivo*.

We used a combination of synthetic siRNA and JC polyoma virus VLPs in living female rats, obtained successful results with an *in vivo* RNAi against an osteoporosis-relevant target, the nuclear kappaB factor ligand RANKL. This target gene is of particular interest since a deregulation of the balance between RANKL and osteoprotegerin toward increased

RANKL levels results in osteoclast formation and pathologic bone resorption.^{3,7,39,40} Intraperitoneal injection of VLPs containing siRNAs against RANKL or fluorophore-conjugated noncognate control RNAs did not cause obvious adverse effects in adult female rats.

VLPs without retargeting for specific cell markers are only able to reach cells that (i) are accessible via the bloodstream, (ii) expose cellular markers including LSTc glycosylation, (iii) express HTR2a. This is true for osteoblasts and osteoblast precursor cells, but not for T-cells, which represent a secondary source of RANKL. Therefore, a maximum effect of 30–40% can be expected for an *in vivo* RNAi approach that is targeting osteoblasts in the living animal.

Silencing of RANKL is dose dependent

Injection of 40 µg or 100 µg (~0.14 to 0.35 mg/kg) of siRNA-loaded VLPs resulted in no or very weak and nonsignificant effects (Figure 4). Reproducible and significant silencing of the target mRNA was achieved by injecting 150 µg VLPs (0.5 mg/kg) containing 11.2 µg siRNAs against RANKL (0.04 mg/kg). However, the amount of injected RNA is relatively low when compared to previous studies that utilized naked siRNA in hydrodynamic tail-vein injections (2.5 to 5 mg/kg), chemically modified siRNAs, or lipid-based technologies (0.3 mg/kg) for *in vivo* delivery.^{41–43} In contrast to other published *in vivo* applications, we achieve significant silencing with smallest quantities for systemic delivery by delivering siRNAs within the VLPs.

Future perspectives

Bone metabolism upon partial silencing of RANKL must be studied in more detail to determine whether a 25–30% knockdown will be sufficient to restore bone stability in ovariectomized female rats as an osteoporosis model.^{44–46} Beneficial effects may be further increased through the delivery of RNAi effectors against RANKL to T-cells, in particular Th17 cells. Also, decreasing the levels of IL-17 may support the recovery of osteoporosis effects.^{47,48} Combining the silencing of RANKL with siRNAs that are directed against the pleckstrin homology domain-containing family O member 1 (*Plekho1*) would also be possible with the VLP-system. This approach has the potential to further improve bone microarchitecture and mechanical properties, as was recently shown for osteoblast-delivered *Plekho1* siRNAs *in vivo*.⁴¹ A rebalancing of RANKL/OPG may alternatively be achieved through increasing OPG levels by means of transgenic (over-) expression. Existing rodent models in mouse and rat indicate that bone mass and stability can be elevated without drastic negative effects.^{49,50} These findings contradict the observation that risks of cardiac disease were increased with serum levels of OPG.^{5,6} A combination of the VLP technology for the careful and moderate knockdown, with conditionally increased OPG levels, would enable a deeper understanding of the pathological mechanisms, down to the cellular and molecular level, which could be applied *in vivo*. One possibility for complementing the partial knockdown of RANKL by VLP-delivered siRNAs is the drug-inducible expression of transgenic OPG from adeno-associated virus backbones. Recombinant adeno-associated viruses have successfully been used in rat animal models to express foreign DNA from

tetracycline-responsive element promoters, where transgenes can be switched on by supplementing doxycycline to the animal's diet.^{51,52} However, at present, the VLP system for *in vivo* delivery can be utilized as a tool with which to study bone metabolism-related questions, as well as using siRNAs to validate potential therapies in the rat.

Materials and methods

Cell culture. Rat calvariae osteoblasts were purchased (Lonza, Basel, Switzerland) and maintained in Dulbecco's Modified Eagle Medium in accordance with the supplier's manual. Differentiation of osteoblasts was initiated prior to treatment of the cells with transfection/transduction reagents. Osteoblast medium for differentiation was made by adding β-Glycerophosphate (10 mmol/l), L-ascorbic acid (50 mg/ml) and 0.01 µmol/l dexamethasone to the standard culture medium. Cells were seeded onto 24-well or 6-well plates at 25,000 to 50,000 cells/ml 24 hours prior to treatment with siRNA-loaded VLPs.

VLP production and loading. JC VP1 DNA was ordered from GENEART as a codon-optimized construct for baculoviral expression and transferred as a *Bam*HI/*Hind*III and *Sph*I/*Nco*I amplicon into the 2× pFBDM vector-based expression system.⁵³ The VP1 gene-containing baculovirus was generated as described by Fitzgerald *et al.*, and expression of VP1 was performed in Hi5 cells according to the manufacturer's manual (Invitrogen, CA).

Viral capsid-containing supernatant was harvested by centrifugation (30 minutes, 10,000 × *g*) and filtered through a 0.45-µm filter. Viral capsids were precipitated by addition of PEG 8000 at room temperature to a final concentration of 7.5% (w/v). Precipitate was separated by centrifugation (30 minutes, 10,000 × *g*) and resuspended in 20 mmol/l HEPES (pH 7.4), containing 150 mmol/l NaCl and 15 mmol/l EGTA and DTT each (dissociation buffer). After 2 hours at room temperature on a tumbling shaker, the remaining precipitate was removed by centrifugation (30 minutes, 21,000 × *g* at 4 °C). Afterwards, the VP1-containing supernatant was dialyzed (MWCO 6–8 kDa) overnight against 5 l of 20 mmol/l HEPES (pH 7.4), containing 150 mmol/l NaCl and 1 mmol/l CaCl₂ (reassembly buffer) at 4 °C under constant stirring. Dialyzed viral capsid-containing samples were centrifuged (30 minutes, 21,000 × *g* at 4 °C) and further purified via size-exclusion chromatography using a Sephacryl S-300 HR gel filtration column connected to a ÄKTA Avant system. The column was equilibrated with reassembly buffer. Viral capsids eluted within the void volume of the column and were concentrated using a Vivaspin column with MWCO 30 kDa (Sartorius, Göttingen, Germany) at 4 °C to the desired concentration of 0.8–1 mg/ml. Empty viral capsids were stored at –80 °C until use.

For transduction, the desired amount of VP1 was incubated in dissociation buffer at room temperature for 30 minutes. Per 25 µg of VP1, 7 µl of a 20 µmol/l siRANKL (J-094995-09 and J-094995-10, GE Healthcare, Little Chalfont, UK) or control RNA (D-001100-01, GE Healthcare or Cy3-labeled control, AM17120, Thermo Fischer Scientific, Waltham, MA) were

added and incubated for another 30 minutes. VP1 was dialyzed against 5 l of reassembly buffer at 4 °C under constant stirring overnight.

Western blot. Sodium dodecyl sulfate gel electrophoresis was performed according to standard protocols. Proteins were separated by standard sodium dodecyl sulfate gel electrophoresis and then transferred onto a nitrocellulose membrane and blocked in TBST (20 mmol/l Tris-HCl, 150 mmol/l NaCl, 0.2% Tween 20, pH 7.4) containing 5% skim milk powder. Antibodies (mouse monoclonal anti-RANKL or mouse monoclonal anti-JCV VP1, both from Abcam, Cambridge, UK) were diluted in the same buffer but with 2.5% skim milk powder and incubated with the membrane for 3 hours at room temperature.

Animals and injections. All animal procedures were approved by the local Animal Care and Use Committee (permission number 33.9-42502-04-11/0560, district authorities of Oldenburg, Germany). The experiments were performed with 3-month-old female Sprague-Dawley rats (Fa Winkelmann, Borcheln, Germany). All rats had approximately the same weight (289 ± 18 g). The rats were kept according to the German animal protection laws and received a standard pellet-diet (ssniff Special Diet, Soest, Germany). All rats were allowed to move freely in their cages. Injections with VLP were applied i.p., i.v., or i.m. depending on the experiments. At the end of the experiments, the rats were euthanized under CO₂ anaesthesia. The sixth lumbar vertebrae, tibiae, and blood samples were removed for analysis.

ELISA analysis of serum samples. An ELISA was used to measure the RANKL content in tibiae samples. For ELISA analysis, we used a standardized ELISA-Kit (SEA855Ra Cloud-Cone, Houston, TX). The assay was performed according to the manufacturer's instructions.

Quantitative PCR. Tibia and lumbar vertebra of all animals were homogenized using a micro-dismembrator S (Sartorius) and mixed with β-mercaptoethanol. Total RNA was extracted using TRIzol reagent (Thermo Fischer Scientific) according to the manufacturer's protocol. Due to the high viscosity of the samples, a prolonged homogenization time (10 minutes) after TRIzol mixing was used. RNA was measured using a Qubit System (Life Technologies, Carlsbad, CA), and reverse transcription was performed with 2,000 ng of total RNA using a SensiFast cDNA Synthesis Kit (Bioline, London, UK). qPCR was performed on an ABI 7500 real-time PCR system (Applied Biosystems, Waltham, MA) using QuantiTect Primer Assays (Qiagen, Hilden, Germany). Relative expression of RANKL (Primer QT00195125) was calculated via the ΔΔCt-method using β-2-microglobulin (QT00176295) as housekeeping gene. 5-HT2a-receptor (HTR2a) qPCR was performed with primers as previously described,⁵⁴ control primers for human β-2-microglobulin were (in 5'–3' direction) B2M-fwd: TGTGCTCGCGCTACTCTCTCT and B2M rev: CGGATGGATGAAACCCAGACA. For rat β-2-microglobulin, the QuantiTect Primer Assay (QT00176295) was used.

Statistical methods. D'Agostino and Pearson test was performed with standardized expression data for RANKL mRNA in the control (and all other) rat samples to evaluate Gaussian distribution.^{27,28,55} A normal distribution was identified for all samples, qualifying the application of the unpaired *t*-test to examine the significance of changes in the treated animals. Mann-Whitney *U*-tests were performed to evaluate significance in unpaired conditions for selected samples. Statistical analyses were performed using PRISM software (GraphPad, CA).

Supplementary material

Figure S1. RT-PCR detects expression of HTR2a (or 5-HT2a receptor) in cells and bone material.

Figure S2. Efficiency of siRNA packaging in VLPs was high for the concentrations used.

Figure S3. VLPs rapidly transduce osteoblast cells and release siRNA cargos for gene silencing.

Figure S4. Individual experimental units (Exp. A and B) show comparable results for qPCR-determined RANKL-levels in bone material from lumbar vertebrae of VLP injected female rats.

Figure S5. RANKL mRNA levels show a broad variation both among individual animals and when comparing data derived from tibiae and lumbar vertebrae.

Figure S6. RANKL ELISA data support qPCR trends without reaching significance.

Table S1. Delivery efficiencies and cell viabilities of rat osteoblasts.

Supplementary Methods

Acknowledgments This study was partially supported by the Elisabeth-Bonhoff Foundation (N 70). We thank Anette Witt and Ramona Castro-Machguth for expert technical assistance and Laura Nothdurft for help with *in vitro* experiments. The authors declare no conflict of interest. The publication of this article was funded by the Open Access fund of the Leibniz Association.

1. Segovia-Silvestre, T, Neutzsky-Wulff, AV, Sorensen, MG, Christiansen, C, Bollerslev, J, Karsdal, MA *et al.* (2009). Advances in osteoclast biology resulting from the study of osteopetrotic mutations. *Hum Genet* **124**: 561–577.
2. Trouvin, AP and Goeb, V (2010). Receptor activator of nuclear factor-κB ligand and osteoprotegerin: maintaining the balance to prevent bone loss. *Clin Interv Aging* **5**: 345–354.
3. Boyce, BF and Xing, L (2007). The RANKL/RANK/OPG pathway. *Curr Osteoporos Rep* **5**: 98–104.
4. Pérez-Sayáns, M, Somoza-Martín, JM, Barros-Angueira, F, Rey, JM and García-García, A (2010). RANK/RANKL/OPG role in distraction osteogenesis. *Oral Surg Oral Med Oral Pathol Oral Radiol Endod* **109**: 679–686.
5. Caidahl, K, Ueland, T and Aukrust, P (2010). Osteoprotegerin: a biomarker with many faces. *Arterioscler Thromb Vasc Biol* **30**: 1684–1686.
6. Omland, T, Ueland, T, Jansson, AM, Persson, A, Karlsson, T, Smith, C *et al.* (2008). Circulating osteoprotegerin levels and long-term prognosis in patients with acute coronary syndromes. *J Am Coll Cardiol* **51**: 627–633.
7. Coetzee, M and Kruger, MC (2004). Osteoprotegerin-receptor activator of nuclear factor-κappaB ligand ratio: a new approach to osteoporosis treatment? *South Med J* **97**: 506–511.
8. Chen, LS, Wang, M, Ou, WC, Fung, CY, Chen, PL, Chang, CF *et al.* (2010). Efficient gene transfer using the human JC virus-like particle that inhibits human colon adenocarcinoma growth in a nude mouse model. *Gene Ther* **17**: 1033–1041.
9. Elbashir, SM, Harborth, J, Lendeckel, W, Yalcin, A, Weber, K and Tuschl, T (2001). Duplexes of 21-nucleotide RNAs mediate RNA interference in cultured mammalian cells. *Nature* **411**: 494–498.

10. Moen, MD and Keam, SJ (2011). Denosumab: a review of its use in the treatment of postmenopausal osteoporosis. *Drugs Aging* **28**: 63–82.
11. Jules, J, Wang, S, Shi, Z, Liu, J, Wei, S and Feng, X (2015). The IVVY motif and tumor necrosis factor receptor-associated factor (TRAF) sites in the cytoplasmic domain of the receptor activator of nuclear factor κ B (RANK) cooperate to induce osteoclastogenesis. *J Biol Chem* **290**: 23738–23750.
12. Elbashir, SM, Lendeckel, W and Tuschl, T (2001). RNA interference is mediated by 21- and 22-nucleotide RNAs. *Genes Dev* **15**: 188–200.
13. Motoyama, K, Mitsuyasu, R, Akao, C, Abu Hashim, II, Sato, N, Tanaka, T et al. (2015). Potential use of thioalkylated mannose-modified dendrimer (G3) α -cyclodextrin conjugate as an NF- κ B siRNA carrier for the treatment of fulminant hepatitis. *Mol Pharm* **12**: 3129–3136.
14. McLendon, JM, Joshi, SR, Sparks, J, Matar, M, Fewell, JG, Abe, K et al. (2015). Lipid nanoparticle delivery of a microRNA-145 inhibitor improves experimental pulmonary hypertension. *J Control Release* **210**: 67–75.
15. Xu, F, Liu, G, Liu, Q, and Zhou, Y (2015). RNA interference of influenza A virus replication by microRNA-adapted lentiviral shRNA. *J Gene Virol* **96**: 2971–2981.
16. Zhang, JM, Wang, Y, Miao, YJ, Zhang, Y, Wu, YN, Jia, LX et al. (2013). Knockout of CD8 delays reendothelialization and accelerates neointima formation in injured arteries of mouse via TNF- α inhibiting the endothelial cells migration. *PLoS One* **8**: e62001.
17. Zhou, HX, Li, XY, Li, FY, Liu, C, Liang, ZP, Liu, S et al. (2014). Targeting RPTP σ with lentiviral shRNA promotes neurites outgrowth of cortical neurons and improves functional recovery in a rat spinal cord contusion model. *Brain Res* **1586**: 46–63.
18. Petry, H, Goldmann, C, Ast, O and Lücke, W (2003). The use of virus-like particles for gene transfer. *Curr Opin Mol Ther* **5**: 524–528.
19. Chang, CF, Wang, M, Ou, WC, Chen, PL, Shen, CH, Lin, PY et al. (2011). Human JC virus-like particles as a gene delivery vector. *Expert Opin Biol Ther* **11**: 1169–1175.
20. Sawa, H and Komagome, R (2005). The JC virus-like particle overlay assay. *Methods Mol Biol* **292**: 175–186.
21. Suzuki, S, Sawa, H, Komagome, R, Orba, Y, Yamada, M, Okada, Y et al. (2001). Broad distribution of the JC virus receptor contrasts with a marked cellular restriction of virus replication. *Virology* **286**: 100–112.
22. Neu, U, Maginnis, MS, Palma, AS, Ströh, LJ, Nelson, CD, Feizi, T et al. (2010). Structure-function analysis of the human JC polyomavirus establishes the LSTc pentasaccharide as a functional receptor motif. *Cell Host Microbe* **8**: 309–319.
23. Dai, SQ, Yu, LP, Shi, X, Wu, H, Shao, P, Yin, GY et al. (2014). Serotonin regulates osteoblast proliferation and function *in vitro*. *Braz J Med Biol Res* **47**: 759–765.
24. Bakker, A and Klein-Nulend, J (2003). Osteoblast isolation from murine calvariae and long bones. *Methods Mol Med* **80**: 19–28.
25. Czekanska, EM, Stoddart, MJ, Richards, RG and Hayes, JS (2012). In search of an osteoblast cell model for *in vitro* research. *Eur Cell Mater* **24**: 1–17.
26. Bustin, SA (2000). Absolute quantification of mRNA using real-time reverse transcription polymerase chain reaction assays. *J Mol Endocrinol* **25**: 169–193.
27. D'Agostino, RB, Belanger, A, and D'Agostino, RBJ (1990). A suggestion for using powerful and informative tests of normality. *The American Statistician* **44**: 316–321.
28. Pearson, ES (1931). Note on tests for normality. *Biometrika* **22**: 423–424.
29. Goldmann, C, Stolte, N, Nisslein, T, Hunsmann, G, Lücke, W and Petry, H (2000). Packaging of small molecules into VP1-virus-like particles of the human polyomavirus JC virus. *J Virol Methods* **90**: 85–90.
30. Lin, MC, Wang, M, Fang, CY, Chen, PL, Shen, CH and Chang, D (2014). Inhibition of BK virus replication in human kidney cells by BK virus large tumor antigen-specific shRNA delivered by JC virus-like particles. *Antiviral Res* **103**: 25–31.
31. Assetta, B, Maginnis, MS, Gracia Ahufinger, I, Haley, SA, Gee, GV, Nelson, CD et al. (2013). 5-HT₂ receptors facilitate JC polyomavirus entry. *J Virol* **87**: 13490–13498.
32. Maginnis, MS, Haley, SA, Gee, GV and Atwood, WJ (2010). Role of N-linked glycosylation of the 5-HT_{2A} receptor in JC virus infection. *J Virol* **84**: 9677–9684.
33. Maginnis, MS, Nelson, CD and Atwood, WJ (2015). JC polyomavirus attachment, entry, and trafficking: unlocking the keys to a fatal infection. *J Neurovirol* **21**: 601–613.
34. Galli, C, Macaluso, G and Passeri, G (2013). Serotonin: a novel bone mass controller may have implications for alveolar bone. *J Negat Results Biomed* **12**: 12.
35. Blizotes, M, Gunness, M, Eshleman, A and Wren, K (2002). The role of dopamine and serotonin in regulating bone mass and strength: studies on dopamine and serotonin transporter null mice. *J Musculoskelet Neuronal Interact* **2**: 291–295.
36. Blizotes, M, Eshleman, A, Burt-Pichat, B, Zhang, XW, Hashimoto, J, Wren, K et al. (2006). Serotonin transporter and receptor expression in osteocytic MLO-Y4 cells. *Bone* **39**: 1313–1321.
37. Warden, SJ, Nelson, IR, Fuchs, RK, Blizotes, MM and Turner, CH (2008). Serotonin (5-hydroxytryptamine) transporter inhibition causes bone loss in adult mice independently of estrogen deficiency. *Menopause* **15**: 1176–1183.
38. Warden, SJ, Robling, AG, Sanders, MS, Blizotes, MM and Turner, CH (2005). Inhibition of the serotonin (5-hydroxytryptamine) transporter reduces bone accrual during growth. *Endocrinology* **146**: 685–693.
39. Morabito, N, Gaudio, A, Lasco, A, Atteritano, M, Pizzoleo, MA, Cincotta, M et al. (2004). Osteoprotegerin and RANKL in the pathogenesis of thalassemia-induced osteoporosis: new pieces of the puzzle. *J Bone Miner Res* **19**: 722–727.
40. Henriksen, K, Bollerslev, J, Everts, V and Karsdal, MA (2011). Osteoclast activity and subtypes as a function of physiology and pathology—implications for future treatments of osteoporosis. *Endocr Rev* **32**: 31–63.
41. Liang, C, Guo, B, Wu, H, Shao, N, Li, D, Liu, J et al. (2015). Aptamer-functionalized lipid nanoparticles targeting osteoblasts as a novel RNA interference-based bone anabolic strategy. *Nat Med* **21**: 288–294.
42. Rettig, GR and Behlke, MA (2012). Progress toward *in vivo* use of siRNAs-II. *Mol Ther* **20**: 483–512.
43. Hu, YB, Li, DG and Lu, HM (2007). Modified synthetic siRNA targeting tissue inhibitor of metalloproteinase-2 inhibits hepatic fibrogenesis in rats. *J Gene Med* **9**: 217–229.
44. Kalu, DN (1991). The ovariectomized rat model of postmenopausal bone loss. *Bone Miner* **15**: 175–191.
45. Johnston, BD and Ward, WE (2015). The ovariectomized rat as a model for studying alveolar bone loss in postmenopausal women. *Biomed Res Int* **2015**: 635023.
46. Netto, CC, Vieira, VC, Marinheiro, LP, Agellon, S, Weiler, H and Maróstica, MR Jr (2012). Are skeletally mature female rats a suitable model to study osteoporosis? *Arq Bras Endocrinol Metabol* **56**: 259–264.
47. Zhao, R (2013). Immune regulation of bone loss by Th17 cells in oestrogen-deficient osteoporosis. *Eur J Clin Invest* **43**: 1195–1202.
48. Graham, LS, Tintut, Y, Parhami, F, Kitchen, CM, Ivanov, Y, Tetradis, S et al. (2010). Bone density and hyperlipidemia: the T-lymphocyte connection. *J Bone Miner Res* **25**: 2460–2469.
49. Wu, Y, Liu, J, Guo, H, Luo, Q, Yu, Z, Liao, E et al. (2013). Establishment of OPG transgenic mice and the effect of OPG on bone microarchitecture. *Int J Endocrinol* **2013**: 125932.
50. Ominsky, MS, Stolina, M, Li, X, Corbin, TJ, Asuncion, FJ, Barrero, M et al. (2009). One year of transgenic overexpression of osteoprotegerin in rats suppressed bone resorption and increased vertebral bone volume, density, and strength. *J Bone Miner Res* **24**: 1234–1246.
51. Payne, KA, Lee, HH, Haleem, AM, Martins, C, Yuan, Z, Qiao, C et al. (2011). Single intra-articular injection of adeno-associated virus results in stable and controllable *in vivo* transgene expression in normal rat knees. *Osteoarthritis Cartilage* **19**: 1058–1065.
52. McGee Santfner, LH, Rendahl, KG, Quiroz, D, Coyne, M, Ladner, M, Manning, WC et al. (2001). Recombinant AAV-mediated delivery of a tet-inducible reporter gene to the rat retina. *Mol Ther* **3**: 688–696.
53. Fitzgerald, DJ, Berger, P, Schaffitzel, C, Yamada, K, Richmond, TJ and Berger, I (2006). Protein complex expression by using multigene baculoviral vectors. *Nat Methods* **3**: 1021–1032.
54. Nau, F Jr, Yu, B, Martin, D and Nichols, CD (2013). Serotonin 5-HT_{2A} receptor activation blocks TNF- α mediated inflammation *in vivo*. *PLoS One* **8**: e75426.
55. Ghasemi, A and Zahediasl, S (2012). Normality tests for statistical analysis: a guide for non-statisticians. *Int J Endocrinol Metab* **10**: 486–489.



This work is licensed under a Creative Commons Attribution-NonCommercial-NoDerivs 4.0 International License. The images or other third party material in this article are included in the article's Creative Commons license, unless indicated otherwise in the credit line; if the material is not included under the Creative Commons license, users will need to obtain permission from the license holder to reproduce the material. To view a copy of this license, visit <http://creativecommons.org/licenses/by-nc-nd/4.0/>

Supplementary Information accompanies this paper on the Molecular Therapy–Nucleic Acids website (<http://www.nature.com/mtna>)